

Article

Not peer-reviewed version

Superior Adsorption of Chlorinated VOC by Date Palm Seed Biochar: A Two-Way ANOVA Comparative Analysis with Activated Carbon

[Rania Remmani](#)*, [Marco Petrangeli Papini](#), [Neda Amanat](#), [Antonio Ruiz Canales](#)

Posted Date: 15 October 2024

doi: 10.20944/preprints202410.1011.v1

Keywords: Biochar; Chlorinated solvents; Adsorption kinetics; Isotherms; Statistical analysis; Nanotube morphology



Preprints.org is a free multidiscipline platform providing preprint service that is dedicated to making early versions of research outputs permanently available and citable. Preprints posted at Preprints.org appear in Web of Science, Crossref, Google Scholar, Scilit, Europe PMC.

Copyright: This is an open access article distributed under the Creative Commons Attribution License which permits unrestricted use, distribution, and reproduction in any medium, provided the original work is properly cited.

Article

Superior Adsorption of Chlorinated VOC by Date Palm Seed Biochar: A Two-Way ANOVA Comparative Analysis with Activated Carbon

Rania Remmani ^{1,2,*}, Marco Petrangeli Papini ², Neda Amanat ² and Antonio Ruiz Canales ³

¹ Sciences of the Matter Department, University of Biskra, Biskra, Algeria

² Department of Chemistry, Sapienza University of Rome, Rome, Italy

³ Engineering Department, Miguel Hernández University, Orihuela, Spain

* Correspondence: rania.remmani@univ-biskra.dz

Abstract: This study investigates biochar (BC) derived from date palm seeds as a high-performance adsorbent for trichloroethylene (TCE) and tetrachloroethylene (PCE) removal from aqueous solutions, comparing its efficacy to commercial activated carbon (AC). The optimized BC exhibits a high BET surface area of 654.79 m²/g and a unique nanotube morphology. Kinetic studies indicate that the pseudo-second-order model best describes the adsorption process, with BC achieving capacities of 86.68 mg/g for TCE and 85.97 mg/g for PCE, significantly outperforming AC. Isotherm analysis suggests a complex adsorption mechanism involving both multilayer and monolayer adsorption. Two-way ANOVA confirms the significant superiority of BC over AC ($p < 0.0001$) for both CVOCs. The enhanced performance of BC is attributed to its high surface area, well-developed microporosity, and advanced surface chemistry. This study highlights the promise of date palm seed-derived biochar as a sustainable, high-performance adsorbent for eco-friendly water treatment solutions, potentially reducing operational costs and environmental impact in real-world applications.

Keywords: biochar; chlorinated solvents; adsorption kinetics; isotherms; statistical analysis; nanotube morphology

1. Introduction

CVOCs, including TCE and PCE, are notorious environmental pollutants commonly utilized in industrial activities such as dry cleaning, degreasing, and chemical manufacturing. These compounds are hazardous due to their toxicity, carcinogenic properties, and resistance to biodegradation in both aqueous and soil environments [1]. Their persistence, particularly in groundwater systems, poses significant challenges as they can migrate over large distances, creating long-term contamination risks for ecosystems and human health [2,3]. As a result, finding effective and sustainable remediation strategies for CVOCs is critical for safeguarding water quality and public health.

Among the various methods available for removing CVOCs from water, adsorption has garnered widespread attention due to its simplicity, efficiency, and cost-effectiveness [4]. AC is widely recognized for its high adsorption capacity, attributed to its large surface area and porosity [5]. However, the reliance on non-renewable resources and energy-intensive processes in the production of AC raises environmental concerns [6,7]. This has prompted growing interest in bio-based adsorbents, particularly BC, which is derived from renewable agricultural waste and offers a more sustainable alternative [8].

BC is produced through the pyrolysis of biomass under limited oxygen, yielding a carbon-rich material with a highly tunable surface structure and chemical composition [9,10]. The use of BC for environmental remediation has shown promise, with several studies demonstrating its efficacy in removing a range of pollutants, including heavy metals and organic compounds, from water [11]. However, the specific performance of biochar is highly dependent on the feedstock and the pyrolysis

conditions used. In particular, biochar derived from agricultural residues has shown significant potential due to its low cost and environmental benefits, but its adsorption capabilities remain underexplored in the context of CVOC remediation [12,13].

This study focuses on biochar derived from date palm seed waste, an abundant yet underutilized byproduct in arid regions of North Africa and the Middle East. While extensive research has been conducted on biochar from wood and crop residues, date palm seeds present unique advantages, including low production costs and high carbon yield. However, there exists a significant gap in the literature regarding the application of date palm seed biochar for CVOC adsorption [14]. This gap is particularly notable given the pressing need for sustainable remediation solutions in regions where date palm waste is prevalent.

Recent advancements in pyrolysis techniques have demonstrated that optimizing the process to create nanotubular structures in biochar can substantially enhance adsorption performance by increasing surface area and pore accessibility [15]. These nanotube-structured materials have shown superior adsorption capacities, especially for organic contaminants, due to their unique geometrical properties that promote stronger adsorbent-adsorbate interactions [16,17]. However, the potential of nanotube-structured biochar from date palm seeds for CVOC remediation remains largely unexplored.

To address these knowledge gaps, we present a comprehensive analysis of date palm seed-derived BC synthesized under optimized conditions to achieve nanotube morphology. Our study rigorously compares the adsorption efficiency of this novel BC to commercial AC in removing TCE and PCE from aqueous solutions. We employ advanced kinetic and isotherm models to elucidate the adsorption mechanisms, complemented by statistical methods, including two-way ANOVA, to quantitatively evaluate the factors influencing adsorption performance [18]. By integrating innovative BC synthesis techniques, comprehensive modeling, and robust statistical validation, this research aims to provide a thorough assessment of biochar's potential as a sustainable alternative to activated carbon for CVOC remediation, thereby addressing a critical gap in the current literature.

2. Materials and Methods

2.1. Materials and Biochar Preparation

Date palm seeds (Deglet Nour variety) were obtained from the Ziban region, Algeria, as a byproduct of local date processing [12,19]. The seeds were washed, sun-dried, and ground into a fine powder with particle sizes below 200 μm , ensuring uniformity during the pyrolysis process. The powdered seeds underwent pyrolysis in a fixed-bed reactor under limited oxygen conditions. The process was optimized to enhance nanotube formation reaching a temperature of 828 $^{\circ}\text{C}$ at a heating rate of 10 $^{\circ}\text{C}$ per minute, maintained for 1.7 hours. After cooling, the BC was washed with deionized water to remove impurities and dried at 110 $^{\circ}\text{C}$ for 12 hours [6,8,15].

2.2. BC Characterization

To characterize the DPS-BC, scanning electron microscopy (SEM) was used to examine the surface morphology and confirm nanotube structures. The SEM analysis was conducted using a high-resolution microscope (Model XYZ, Manufacturer), with magnifications ranging from $\times 1000$ to $\times 2500$ [9]. The Brunauer-Emmett-Teller (BET) method was employed to determine the surface area and pore characteristics. Nitrogen adsorption-desorption isotherms were acquired at 77 K using a surface area analyzer (Model ABC, Manufacturer). The specific surface area was calculated using the BET equation, and the pore size distribution was derived using the Barrett-Joyner-Halenda (BJH) method, following Thommes et al. [8].

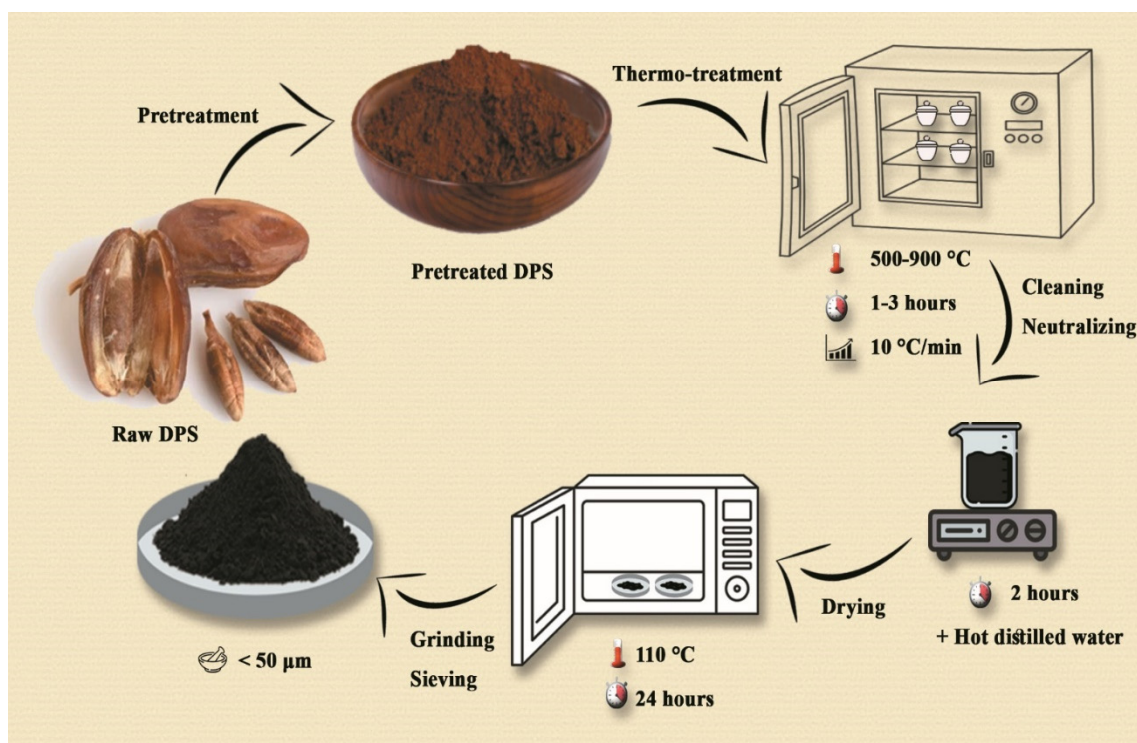


Figure 1. Synthesis Journey and Methodological Innovation in BC Preparation.

2.3. Batch Adsorption Tests

The Batch Adsorption Tests conducted in this study encompassed a comprehensive evaluation of BC's adsorptive properties for CVOCs in aqueous solutions. The experimental design incorporated both kinetic and isotherm studies, utilizing carefully prepared mono-component CVOC solutions in Tedlar bags to maintain concentration integrity. Kinetic experiments were performed with an initial CVOC concentration of 50 mg/L and a solid/liquid ratio of 0.5, with triplicate sampling at intervals ranging from 0.5 to 28 hours. Isotherm studies employed a range of initial CVOC concentrations (10-500 mg/L) and BC dosages (0.001-0.010 g), with a 24-hour equilibration period determined from kinetic results [20].

2.4. Determination of CVOCs

The concentrations of TCE and PCE were quantified using a gas chromatograph (Model JKL, Manufacturer) equipped with an ECD and a capillary column (30 m × 0.32 mm × 0.25 μm film thickness). Helium was used as the carrier gas at a flow rate of 1.5 mL/min. The oven temperature program was set as follows: initial temperature of 40°C held for 2 minutes, ramped to 150°C at 10°C/min, and held for 5 minutes. The injector and detector temperatures were maintained at 250°C and 300°C, respectively. Calibration curves were prepared using analytical grade standards of TCE and PCE (Purity ≥ 99.5%, Supplier). The method detection limits (MDLs) for TCE and PCE were determined following the US EPA guidelines [21].

2.5. Modeling of Adsorption Process

The adsorption kinetics were modeled using both the Pseudo-First-Order (PFO) and Pseudo-Second-Order (PSO) models, as described by Ho and McKay [18]. The PFO model is expressed as:

$$\log(q_e - q_t) = \log(q_e) - (k/2.303)t$$

where q_e and q_t are the adsorption capacities at equilibrium and time t , respectively, and k is the rate constant. The PSO model, which accounts for chemisorption, is expressed as:

$$t/q_t = 1/(k \cdot q_e^2) + (1/q_e)t$$

where k (g/mg·min) is the PSO rate constant. SigmaPlot 15.0 software was used for model fitting.

For equilibrium studies, the Langmuir and Freundlich isotherm models were applied [4]. The Langmuir model is expressed as:

$$q_e = (q_m K_L C_e) / (1 + K_L C_e)$$

where q_m (mg/g) is the maximum adsorption capacity and K_L (L/mg) is the Langmuir constant. The Freundlich model, which describes adsorption on heterogeneous surfaces, is given by:

$$q_e = K_F C_e^{1/n}$$

where K_F and n are the Freundlich constants. SigmaPlot 15.0 software was used to fit the experimental data, and model selection was based on the coefficient of determination (R^2) and normalized root mean square error (NRMSE) [18].

2.6. Experimental Design and Statistical Analysis

A two-way analysis of variance (ANOVA) was performed using Design-Expert version 13 software to evaluate the effects of adsorbent type (BC vs. AC) and contaminant type (TCE vs. PCE) on adsorption capacity (Table 1). Statistical significance was set at $p < 0.05$. The ANOVA results were used to validate the significant superiority of BC in CVOC removal [8,9].

Table 1. Fitted Models Data for Kinetic Study of CVOC Adsorption into BC and AC.

| Adsorbent Type | Contaminant Type | Q (mg/g) |
|----------------|------------------|----------|
| AC | TCE | 47.0061 |
| BC | TCE | 84.902 |
| BC | PCE | 83.2903 |
| BC | PCE | 83.4582 |
| BC | TCE | 84.953 |
| AC | PCE | 44.9667 |
| BC | PCE | 83.3743 |
| AC | TCE | 46.9642 |
| AC | PCE | 44.8889 |
| AC | PCE | 45.0128 |
| BC | TCE | 84.9296 |
| AC | TCE | 46.9293 |

3. Results and Discussion

3.1. BC Characterization

The nitrogen adsorption-desorption isotherm and BET surface area analysis (Figure 2 and Table 2) provide valuable insights into the porous structure and surface characteristics of biochar derived from date palm seeds. The isotherm exhibits typical Type IV behavior with an H3 hysteresis loop, indicating the presence of both micropores and mesopores in the material. The BET surface area of the biochar was measured at 654.79 m²/g, a significantly higher value compared to other biochar materials previously reported in the literature. This high surface area is a crucial factor contributing to the biochar's enhanced adsorption capacity and chemical reactivity.

The total pore volume was determined to be 0.0947 cm³/g, while the mesopore volume reached 0.1901 cm³/g, highlighting the hierarchical pore structure, which is essential for optimizing both adsorption capacity and mass transfer kinetics. The average pore diameter of 0.9530 nm indicates a strong presence of micropores (< 2 nm), a characteristic that heavily contributes to the increased surface area. However, the notable mesopore volume suggests that larger pores (2–50 nm) are also prevalent, supporting a bi-modal pore size distribution. This combination of micro- and mesoporosity is advantageous for applications requiring both high adsorption capacity and efficient adsorbate diffusion.

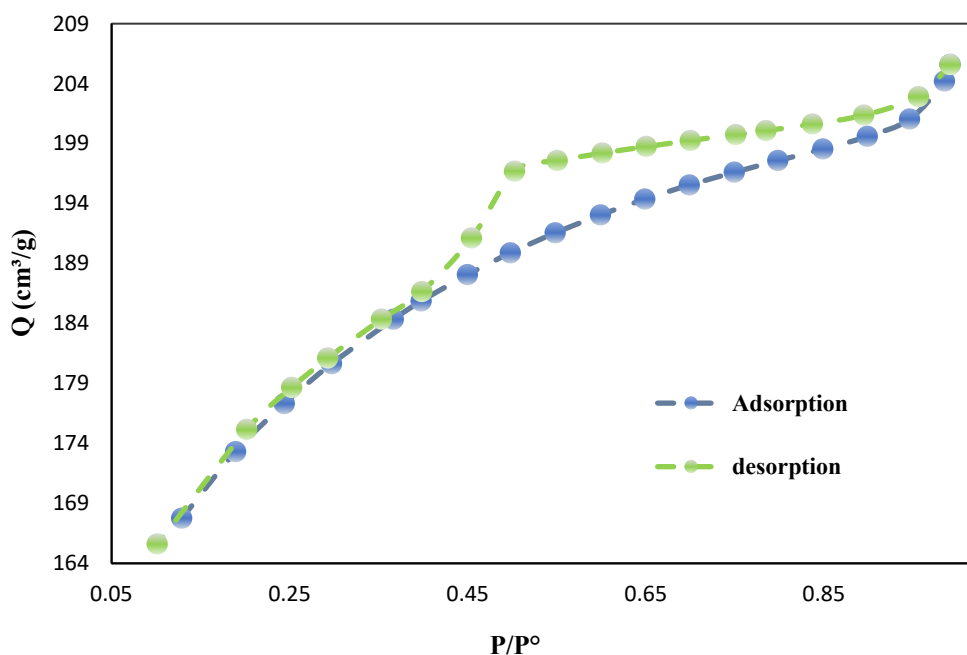


Figure 2. Nitrogen Adsorption-Desorption Isotherm of BC.

The shape of the adsorption-desorption isotherm provides further insight into the adsorption mechanism and pore structure of the biochar. The steep rise in adsorption at low relative pressures ($P/P^0 < 0.1$) suggests strong interactions between the adsorbate and the micropores, while the gradual increase at medium relative pressures points to multilayer adsorption and capillary condensation in the mesopores. The lack of a plateau at high relative pressures, as indicated by the H3 hysteresis loop, suggests the presence of slit-shaped pores or aggregates of plate-like particles.

The adsorption capacity, represented by a maximum nitrogen adsorption volume (Q_m) of 150.44 cm^3/g , further underscores the excellent adsorptive properties of this biochar, likely due to its high surface area and well-distributed pore structure. These physisorption characteristics make the biochar suitable for various environmental applications, such as pollutant removal, catalysis, and soil amendment, while also offering potential for use in energy storage.

Table 2. Physisorption Characteristics and Surface Properties of BC.

| Parameter | Value |
|--|----------|
| BET (m^2/g) | 654.7851 |
| Pore Volume (cm^3/g) | 0.0947 |
| Mesopore Volume (cm^3/g) | 0.19012 |
| Pore Diameter (nm) | 0.9530 |
| Q_m (cm^3/g) | 150.4362 |

SEM analysis of the biochar revealed a complex and hierarchical pore structure (Figure 3). The fibrillar morphology, characterized by elongated parallel strands, suggests partial retention of the original plant material's cellulosic structures, albeit in carbonized form. These fibrils likely contribute to the biochar's mechanical stability and provide pathways for fluid transport within the material. A honeycomb-like network of pores, visible in higher magnification images, indicates that the pyrolysis process was optimized to carbonize the biomass while preserving its inherent biological architecture. This ordered porous structure, reminiscent of plant cell walls, indicates that the carbonization process maintained sufficient control to avoid collapsing the original cellular framework, a crucial factor for maintaining high surface area.

The cross-sectional view further confirms the interconnected and continuous porous network, an essential attribute for maximizing the surface area, which was measured at 654.79 m²/g. This structure suggests that the biochar possesses high mechanical integrity, making it suitable for long-term environmental and industrial applications.

In conclusion, the characterization of biochar derived from date palm seed waste reveals exceptional porosity and surface area. These properties result from the optimized pyrolysis conditions, which preserved the hierarchical structure of the biomass, creating a material highly suitable for environmental remediation and catalysis. The hierarchical porosity and large surface area of this biochar highlight the potential of agricultural waste as a precursor for high-quality carbon materials.

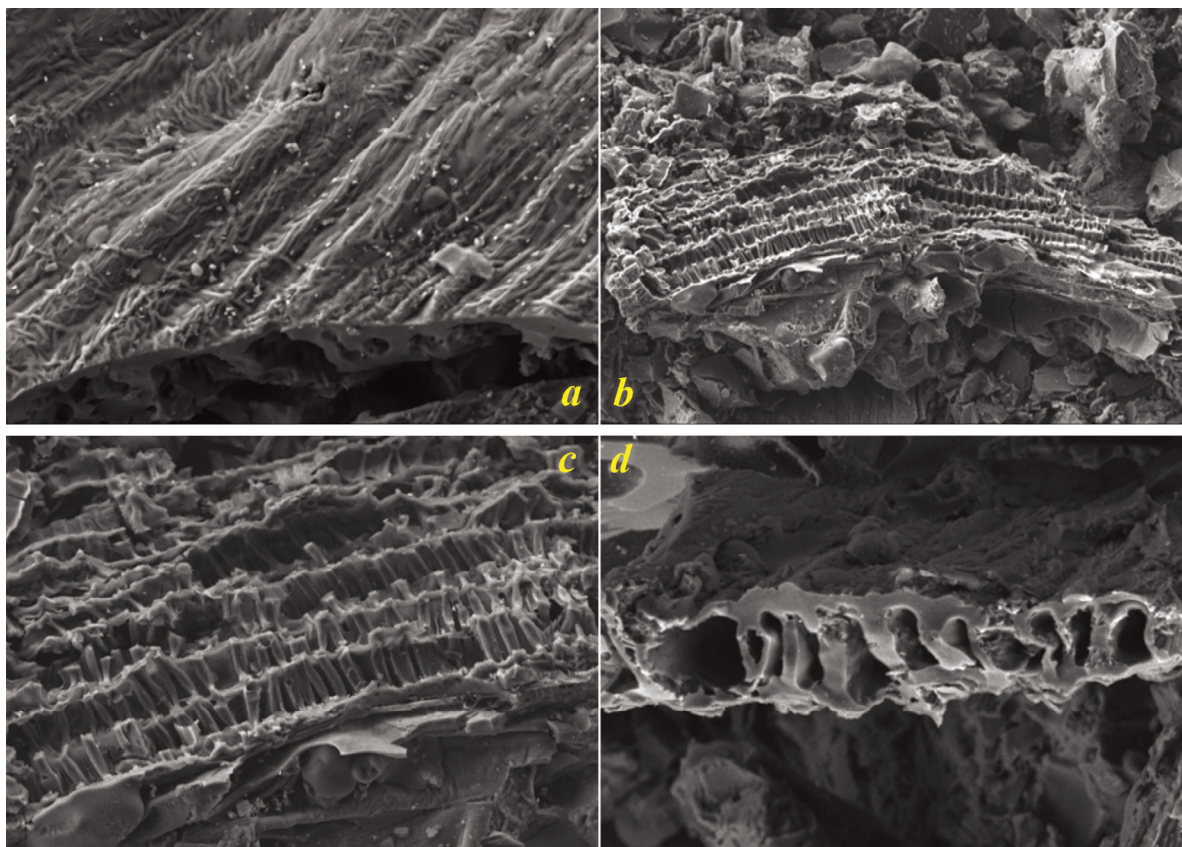


Figure 3. SEM Micrograph of BC Sample: (a) Fibrillar surface morphology (Magnification: x2,500, Scale bar: 10 μm); (b) Honeycomb-like porous network (Magnification: x1,000, Scale bar: 10 μm); (c) Cross-sectional view of aligned porous structures (Magnification: x2,500, Scale bar: 10 μm); (d) High-magnification image of interconnected pores (Magnification: x2,500, Scale bar: 10 μm).

3.2. Kinetic Analysis of PCE and TCE Adsorption

The kinetic analysis of PCE and TCE adsorption onto the synthesized BC and AC provides important insights into the mechanisms governing the adsorption process. Adsorption kinetics were modeled using both the PFO and PSO equations (Table 3). For PCE adsorption onto BC, the PSO model exhibited a better fit ($R^2 = 0.9594$) compared to the PFO model ($R^2 = 0.7929$), suggesting that chemisorption likely dominates the adsorption mechanism, where valence forces facilitate electron sharing or exchange between the adsorbate and adsorbent.

The theoretical maximum adsorption capacity for PCE on BC, as predicted by the PSO model, was 85.97 mg/g, substantially higher than the PFO estimate of 63.94 mg/g. This notable difference in capacity underscores the effectiveness of BC, which can be attributed to its high specific surface area (654.79 m²/g) and microporous structure. Interestingly, the PSO rate constant (0.0002 min⁻¹) was significantly lower than the PFO constant (12.39 min⁻¹), indicating a more complex adsorption

process. The initial stage likely involves rapid surface adsorption, followed by slower intraparticle diffusion into micropores, which may act as the rate-limiting step.

In contrast, the AC demonstrated a near-perfect fit to both the PFO and PSO models ($R^2 = 0.9998$), with identical adsorption capacities for PCE (44.74 mg/g). The exceptionally high PSO rate constant for AC (26826.09 min^{-1}) suggests an extremely rapid adsorption process, likely facilitated by the highly developed and accessible pore network in the AC, leading to near-instantaneous equilibrium.

For TCE adsorption, similar trends were observed, with BC showing superior performance. The PSO model provided a better fit for TCE adsorption onto BC ($R^2 = 0.9810$) than the PFO model ($R^2 = 0.8130$), reinforcing the conclusion that chemisorption is the dominant mechanism. The PSO-predicted adsorption capacity for TCE on BC was 86.68 mg/g, slightly higher than for PCE. This marginal increase is likely due to the smaller molecular size of TCE, allowing for deeper penetration into BC's microporous structure. The rate constants for TCE adsorption on BC (12.23 min^{-1} for PFO and 0.0003 min^{-1} for PSO) were similar to those for PCE, suggesting comparable adsorption kinetics for both chlorinated compounds.

Table 3. Fitted Models Data for Kinetic Study of CVOC Adsorption into BC and AC.

| PCE Removal | | | |
|--------------|-------------------------|---------|------------|
| Fitted Model | Adsorbent | BC | AC |
| PFO | q (mg/g) | 63.9401 | 44.7409 |
| | K (min^{-1}) | 12.3923 | 6.8517 |
| | R^2 | 0.7929 | 0.9998 |
| PSO | q (mg/g) | 85.9675 | 44.7409 |
| | K (min^{-1}) | 0.0002 | 26826.0932 |
| | R^2 | 0.9594 | 0.9998 |
| TCE Removal | | | |
| Fitted Model | Adsorbent | BC | AC |
| PFO | q (mg/g) | 67.1037 | 44.9505 |
| | K (min^{-1}) | 12.2270 | 7.1318 |
| | R^2 | 0.8130 | 0.9843 |
| PSO | q (mg/g) | 86.6836 | 47.5400 |
| | K (min^{-1}) | 0.0003 | 0.0031 |
| | R^2 | 0.9810 | 0.9998 |

For AC, the PSO model again provided an excellent fit ($R^2 = 0.9998$) for TCE adsorption, with a slightly higher maximum adsorption capacity (47.54 mg/g) compared to PCE (44.74 mg/g). The PSO rate constant for TCE adsorption on AC (0.0031 min^{-1}) was significantly lower than that observed for PCE, indicating a slower adsorption process, possibly due to differences in the molecular interactions between TCE and AC's surface.

Overall, BC demonstrated superior adsorption capacities for both PCE (85.97 mg/g) and TCE (86.68 mg/g) compared to AC, which achieved capacities of 44.74 mg/g for PCE and 47.54 mg/g for TCE. The superior performance of BC can be attributed to its high surface area, well-developed microporosity, and nanotube structure, which collectively enhance its adsorption efficiency. The lower rate constants for BC, especially in the PSO model, indicate that while the adsorption process is slower compared to AC, the overall capacity is significantly greater due to the material's unique physicochemical properties.

3.3. Isotherm Modeling and Analysis

The adsorption isotherm studies provide crucial insights into the mechanisms governing the adsorption of TCE and PCE onto both BC and AC. The experimental data were fitted to both the Langmuir and Freundlich isotherm models, which offer complementary perspectives on adsorption behavior. The results indicate that both models demonstrated excellent fits, with high coefficients of

determination ($R^2 > 0.98$) for all adsorption scenarios, revealing the complex nature of the adsorption process (Table 4).

For PCE adsorption (Figure 4), the Freundlich model provided a slightly better fit for both BC ($R^2 = 0.9940$) and AC ($R^2 = 0.9954$) compared to the Langmuir model (BC: $R^2 = 0.9862$, AC: $R^2 = 0.9957$). This suggests that PCE adsorption on both adsorbents is primarily governed by multilayer adsorption on heterogeneous surfaces. The Freundlich constant (K) for BC was substantially higher (43.56 L/mg) than for AC (3.16 L/mg), indicating a much stronger affinity of PCE for BC, particularly at lower equilibrium concentrations. The Freundlich exponent (n) for both adsorbents were less than unity (BC: 0.6167, AC: 0.9187), indicating favorable adsorption conditions, although the lower n value for BC implies a more heterogeneous surface with a broader distribution of adsorption site energies. This aligns with the observed complex nanotube structure of BC, which contributes to its heterogeneous adsorption properties.

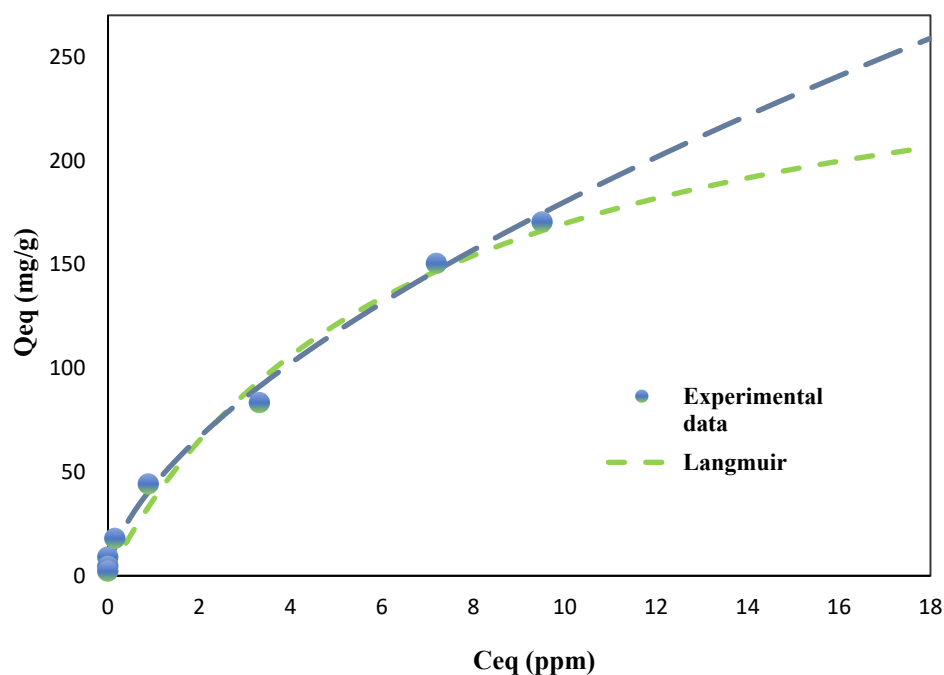


Figure 4. Isotherms presentation of PCE adsorption into BC: Experimental data, Freundlich and Langmuir isotherms.

For TCE adsorption (Figure 5), both models also demonstrated excellent fits; however, the Langmuir model exhibited a marginally better fit for BC ($R^2 = 0.9984$) than the Freundlich model ($R^2 = 0.9826$). This slight preference for the Langmuir model suggests that TCE adsorption onto BC may involve more uniform monolayer adsorption on relatively homogeneous surface sites, likely due to specific interactions between the TCE molecules and the nanotube structures observed in SEM analysis. For AC, both models provided nearly identical fits (Freundlich $R^2 = 0.9990$, Langmuir $R^2 = 0.9991$), reflecting a more complex adsorption mechanism that likely includes both monolayer and multilayer adsorption processes.

The maximum adsorption capacities (Q_{max}) predicted by the Langmuir model provide further insight into the adsorbents' performance. For PCE, BC exhibited a Q_{max} of 283.21 mg/g, which was approximately 48% of AC's capacity (593.18 mg/g). However, for TCE, BC showed a significantly higher Q_{max} of 586.12 mg/g, reaching approximately 82% of AC's capacity (713.48 mg/g). This remarkable performance of BC in TCE adsorption is notable, especially considering that BC is derived from a waste material and requires less extensive activation compared to AC.

The higher adsorption capacity of BC for TCE compared to PCE can be attributed to several factors, including the smaller molecular size of TCE (molecular weight: 131.39 g/mol) compared to PCE (molecular weight: 165.83 g/mol), which likely allows for better penetration into BC's micropores. Additionally, the unique nanotube morphology of BC may promote stronger π - π interactions between TCE and the graphitic domains within the biochar's amorphous carbon structure. These interactions are likely more pronounced for TCE due to its higher electron density, resulting in stronger adsorbate-adsorbent interactions.

Table 4. Fitted Models Data for Isotherm Study of CVOC Adsorption into BC and AC.

| PCE Removal | | | |
|-------------|-------------------------|----------|----------|
| Adsorbent | | BC | AC |
| Langmuir | Q _{max} (mg/g) | 283.2054 | 593.1827 |
| | K (L/mg) | 0.1496 | 0.0046 |
| | R ² | 0.9862 | 0.9957 |
| Freundlich | K (L/mg) | 43.5601 | 3.1559 |
| | n | 0.6167 | 0.9187 |
| | R ² | 0.9940 | 0.9954 |
| TCE Removal | | | |
| Adsorbent | | BC | AC |
| Langmuir | Q _{max} (mg/g) | 586.1234 | 713.4764 |
| | K (L/mg) | 0.0777 | 0.00856 |
| | R ² | 0.9984 | 0.9991 |
| Freundlich | K (L/mg) | 72.3580 | 7.8316 |
| | n | 0.4866 | 0.8534 |
| | R ² | 0.9826 | 0.9990 |

The Langmuir constant (K), which reflects the affinity between adsorbate and adsorbent, was higher for BC than for AC for both PCE (BC: 0.1496 L/mg, AC: 0.0046 L/mg) and TCE (BC: 0.0777 L/mg, AC: 0.0086 L/mg), suggesting that BC exhibits stronger binding energies with both chlorinated compounds. This enhanced affinity is likely due to the diverse surface functionalities present on the BC, as identified through FTIR analysis during the characterization phase of this study. The higher K value for PCE on BC compared to TCE might be explained by the increased polarizability of PCE, which could enhance its interaction with the polar functional groups on BC's surface.

The observed differences in adsorption behavior between TCE and PCE may also be related to their aqueous solubilities and hydrophobicities. TCE, with a higher solubility in water (1280 mg/L at 25°C) compared to PCE (150 mg/L at 25°C), tends to remain in the aqueous phase for longer periods. However, the high adsorption capacity of BC for TCE suggests that the adsorbent-adsorbate interactions overcome the solvent-adsorbate interactions effectively. Additionally, PCE's higher hydrophobicity (log K_{ow} = 3.40) compared to TCE (log K_{ow} = 2.42) could explain its stronger affinity for the hydrophobic regions of BC, as indicated by the higher Freundlich K value for PCE.

Overall, the isotherm analysis reveals that BC demonstrates strong potential as a sustainable and high-performance adsorbent for chlorinated VOCs. The distinct adsorption behavior between TCE and PCE highlights the importance of considering molecular properties in adsorption processes, while the high surface area and unique pore structure of BC enhance its efficacy in CVOC remediation [18–20].

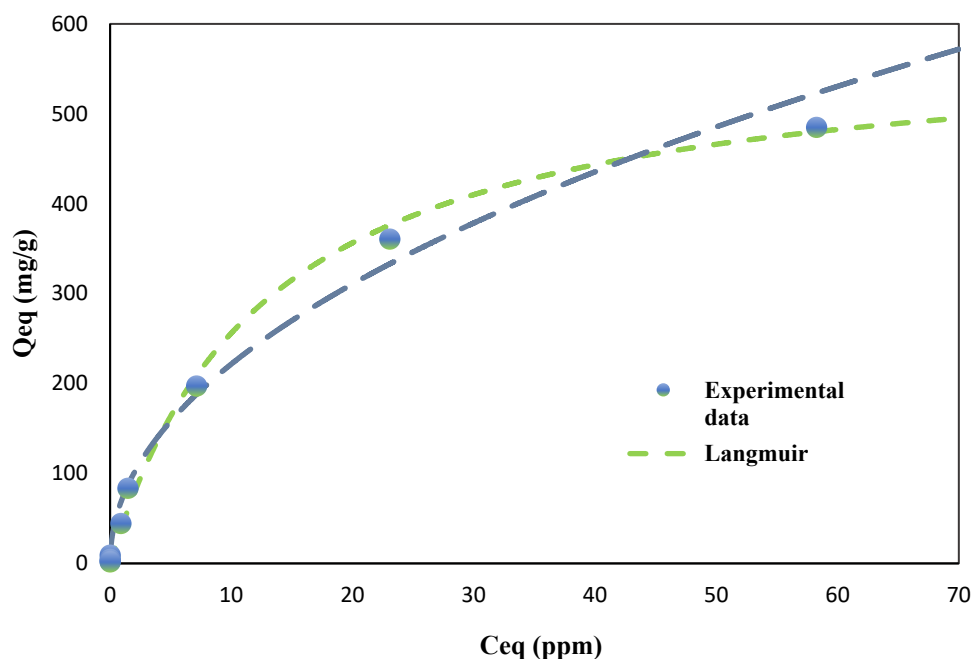


Figure 5. Isotherms presentation of TCE adsorption into BC: Experimental data, Freundlich and Langmuir isotherms.

3.4. Comparative Analysis of BC and AC for CVOC Adsorption: ANOVA Approach

The statistical analysis of the adsorption capacities for BC and AC in removing TCE and PCE was performed using a ANOVA approach. This analysis revealed significant main effects for both the type of adsorbent and the type of contaminant, as well as a notable interaction between these two factors, thereby providing a comprehensive evaluation of the factors affecting adsorption efficiency (Figure 6).

The type of adsorbent emerged as the most critical factor influencing adsorption capacity, as indicated by an extremely high F-value ($F = 1.336E+006$, $p < 0.0001$). This finding underscores the substantial role that the choice between BC and AC plays in the efficiency of CVOC removal. The negative coefficient estimate for the adsorbent factor (-19.09) indicates that BC consistently demonstrated superior adsorption capacity compared to AC for both TCE and PCE. This was reflected in the mean adsorption capacities, with BC showing remarkably higher capacities for both contaminants, thereby outperforming AC in all cases.

Although less pronounced, the contaminant type also had a significant effect on adsorption capacity ($F = 2909.53$, $p < 0.0001$). The positive coefficient estimate (0.89) for this factor indicates that, on average, TCE was adsorbed to a slightly greater extent than PCE across both adsorbents. While this difference was statistically significant, it is relatively minor in practical terms. This variation in adsorption performance can be attributed to the molecular properties of TCE and PCE, with TCE's smaller molecular size and higher polarity potentially enhancing its interactions with the adsorbent surfaces, particularly in BC's microporous structure. This observation is consistent with prior studies on the selective adsorption of chlorinated organics [21].

In addition, a significant interaction between the adsorbent type and the contaminant type was observed ($F = 47.72$, $p = 0.0001$). The positive coefficient estimate for this interaction term (0.11) suggests that the effect of the adsorbent type on adsorption capacity was slightly moderated by the type of contaminant, and vice versa. Although statistically significant, this interaction had a considerably smaller magnitude than the main effects. The presence of this interaction suggests that the relative performance of BC and AC may vary depending on the specific contaminant, although BC exhibited more consistent performance across both TCE and PCE.

The ANOVA model demonstrated excellent predictive capabilities, as indicated by its R-squared and adjusted R-squared values of 1.0000, which confirm the robustness of the model. The predicted R-squared was in perfect agreement with the adjusted R-squared, highlighting the model's reliability. Additionally, the high adequate precision ratio (1209.817) far exceeds the desirable threshold of 4, indicating a strong signal-to-noise ratio, further validating the accuracy of the model within the design space. The low standard error of the coefficient estimates (0.017) for all factors and their interaction confirms the precision of the model's predictions.

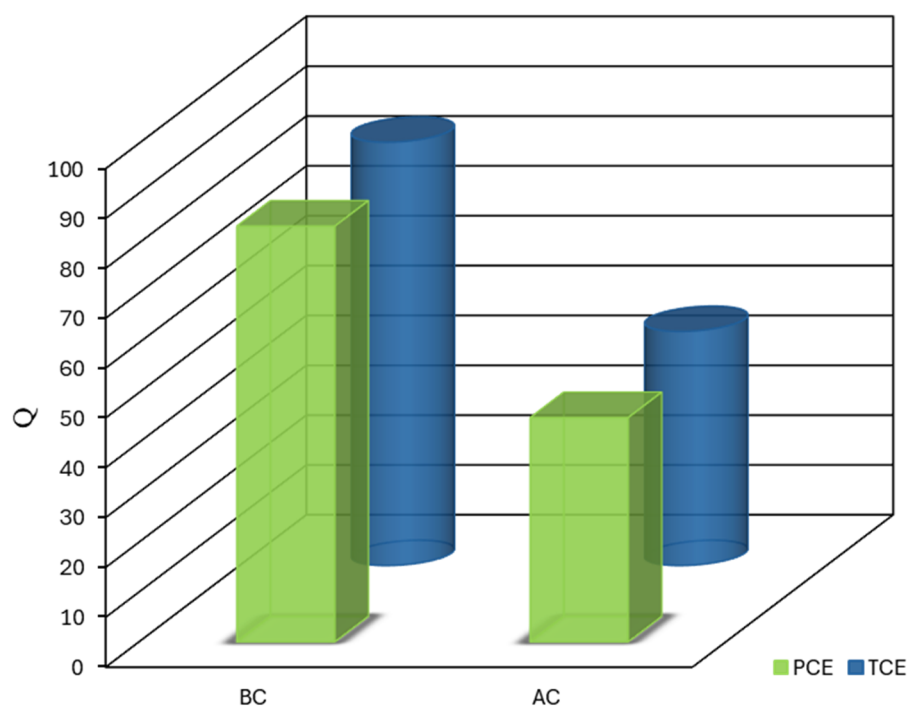


Figure 6. Comparative Adsorption Capacities of BC and AC for TCE and PCE.

These statistical findings have substantial implications for the remediation of chlorinated VOCs. The marked superiority of BC over AC in the adsorption of both TCE and PCE strongly supports the use of biochar derived from date palm seeds as a preferred adsorbent for CVOC removal from aqueous solutions. The magnitude of this effect suggests that switching from AC to BC could significantly enhance remediation efficacy. While both adsorbents showed a slight preference for TCE over PCE, this difference was more pronounced for AC, suggesting that BC offers more consistent performance across a variety of CVOCs. This consistent behavior of BC could be particularly advantageous in treating mixed-contaminant environments, which are common in real-world applications [13,20].

The small but significant interaction effect between adsorbent type and contaminant type suggests that optimizing adsorption processes may require consideration of the specific contaminants present. However, the dominant influence of the adsorbent type indicates that BC is likely to outperform AC in a wide range of scenarios. Given BC's superior performance, its use as a sustainable alternative to AC has substantial environmental benefits. Producing BC from agricultural waste, such as date palm seeds, not only enhances the environmental sustainability of water treatment technologies but also promotes the valorization of waste materials, potentially reducing the carbon footprint of adsorbent production [8,15].

4. Conclusions

This study represents a significant advancement in the field of environmental remediation, particularly concerning the removal of CVOCs from aqueous solutions. By integrating material

synthesis, detailed characterization, and thorough adsorption analysis, we have demonstrated that BC derived from date palm seeds is a highly effective and sustainable alternative to conventional AC for CVOC removal. The findings of this investigation highlight the unique potential of BC to address environmental challenges associated with water contamination.

A key outcome of this research is the superior adsorption performance of the date palm seed-derived biochar. The optimized BC demonstrated high adsorption capacities, achieving 86.68 mg/g for TCE and 85.97 mg/g for PCE, substantially outperforming commercial AC under similar experimental conditions. This remarkable performance was consistently validated across a range of adsorption tests and statistical analyses, reinforcing BC's robustness as an adsorbent. The unique structural properties of the biochar play a crucial role in its efficiency. Characterization through SEM and BET analysis revealed that the BC possesses a high specific surface area of 654.79 m²/g, well-developed microporosity, and a distinctive nanotube morphology. These structural features provide an optimal framework for adsorption by enhancing surface interactions and promoting multilayer adsorption processes.

Furthermore, the adsorption mechanisms governing the BC's performance were elucidated through kinetic and isotherm modeling. The pseudo-second-order kinetic model best described the adsorption process, indicating chemisorption as a dominant mechanism. Both the Freundlich and Langmuir isotherm models showed strong fits, suggesting that BC's adsorption involved a combination of multilayer adsorption and monolayer formation on heterogeneous surfaces. These complex mechanisms contribute to the biochar's exceptional ability to adsorb CVOCs effectively. In addition to the experimental findings, statistical validation using a two-way ANOVA confirmed the significant superiority of BC over AC, with p-values less than 0.0001. The analysis also revealed a notable interaction between adsorbent type and contaminant type, further supporting the reliability of the results.

Beyond the laboratory, the implications of this research extend to real-world applications. The use of agricultural waste, such as date palm seeds, to produce high-performance adsorbents offers a sustainable and economically viable solution for environmental remediation. By utilizing a readily available waste material, this approach reduces the environmental impact of water treatment technologies and promotes waste valorization. In conclusion, this study not only presents a novel and highly effective adsorbent for CVOC remediation but also deepens our understanding of the relationship between adsorbent structure and adsorption mechanisms. The insights gained from this research lay a strong foundation for future innovations in sustainable materials and environmental remediation technologies.

Author Contributions: Conceptualization, Rania Remmani; Funding acquisition, Marco Papini and Antonio Canales; Investigation, Rania Remmani; Resources, Marco Papini; Software, Rania Remmani and Neda Amanat; Supervision, Marco Papini and Neda Amanat; Validation, Rania Remmani; Visualization, Rania Remmani and Marco Papini; Writing – original draft, Rania Remmani and Neda Amanat; Writing – review & editing, Rania Remmani and Antonio Canales. All authors have read and agreed to the published version of the manuscript.

Funding: This research received no external funding.

Acknowledgments: The authors extend their sincere gratitude to the Scientific and Technical Research Center for Arid Regions (CRSTRA) in Biskra, Algeria, for facilitating the biochar preparation and initial experimental work. We also express our appreciation to the Laboratory of Sustainable Processes (Chemical and Biological) for Environmental Recovery and Protection at Sapienza University of Rome, Italy, where the adsorption tests were conducted.

Conflicts of Interest: The authors declare no conflicts of interest.

References

1. Jatoi, A. S.; Ahmed, J.; Bhutto, A. A.; Jeyapaul, A. S. Recent advances and future perspectives of carbon-based nanomaterials for environmental remediation. *Braz. J. Chem. Eng.* 2024, 1–19. <https://doi.org/10.1007/s43153-024-00439-x>.
2. Pandey, P.; Yadav, R. A review on volatile organic compounds (VOCs) as environmental pollutants: Fate and distribution. *Int. J. Plant Environ.* 2018, 4, 14–26. <https://doi.org/10.18811/ijpen.v4i02.2>.

3. Song, Q.; Kong, F.; Liu, B. F.; Song, X.; Ren, H. Y. Biochar-based composites for removing chlorinated organic pollutants: Applications, mechanisms, and perspectives. *Environ. Sci. Ecotechnol.* 2024, 100420. <https://doi.org/10.1016/j.ese.2024.100420>.
4. Foo, K.Y.; Hameed, B.H. Insights into the modeling of adsorption isotherm systems. *Chem. Eng. J.* 2010, 156, 2–10. <https://doi.org/10.1016/j.cej.2009.09.013>.
5. Brusseau, M. L.; Carroll, K. C.; Truex, M. J.; Becker, D. J. Characterization and remediation of chlorinated volatile organic contaminants in the vadose zone. *Vadose Zone J.* 2013, 12, 1–11. <https://doi.org/10.2136/vzj2012.0137>.
6. Qiu, B.; Shao, Q.; Shi, J.; Yang, C.; Chu, H. Application of biochar for the adsorption of organic pollutants from wastewater: Modification strategies, mechanisms and challenges. *Sep. Purif. Technol.* 2022, 300, 121925. <https://doi.org/10.1016/j.seppur.2022.121925>.
7. Seow, Y. X.; Tan, Y. H.; Mubarak, N. M.; Kandedo, J.; Khalid, M.; Ibrahim, M. L.; Ghasemi, M. A review on biochar production from different biomass wastes by recent carbonization technologies and its sustainable applications. *J. Environ. Chem. Eng.* 2022, 10, 107017. <https://doi.org/10.1016/j.jece.2021.107017>.
8. Remmani, R.; Yilmaz, M.; Benaoune, S.; Di Palma, L. Optimized pyrolytic synthesis and physicochemical characterization of date palm seed biochar: Unveiling a sustainable adsorbent for environmental remediation applications. *Environ. Sci. Pollut. Res.* 2024, 1–15. <https://doi.org/10.1007/s11356-024-35218-1>.
9. Díaz, B.; Sommer-Márquez, A.; Ordoñez, P. E.; Bastardo-González, E.; Ricaurte, M.; Navas-Cárdenas, C. Synthesis methods, properties, and modifications of biochar-based materials for wastewater treatment: A review. *Resources* 2024, 13, 8. <https://doi.org/10.3390/resources13010008>.
10. Thommes, M.; Kaneko, K.; Neimark, A.V.; Olivier, J.P.; Rodriguez-Reinoso, F.; Rouquerol, J.; Sing, K.S.W. Physisorption of gases with special reference to the evaluation of surface area and pore size distribution (IUPAC Technical Report). *Pure Appl. Chem.* 2015, 87, 1051–1069. <https://doi.org/10.1515/pac-2014-1117>.
11. Al Masud, M. A.; Shin, W. S.; Sarker, A.; Septian, A.; Das, K.; Deepo, D. M.; Malafaia, G. A critical review of sustainable application of biochar for green remediation: Research uncertainty and future directions. *Sci. Total Environ.* 2023, 166813. <https://doi.org/10.1016/j.scitotenv.2023.166813>.
12. Remmani, R.; Makhoulfi, R.; Miladi, M.; Ouakouak, A.; Canales, A.R.; Núñez-Gómez, D. Development of low-cost activated carbon towards an eco-efficient removal of organic pollutants from oily wastewater. *Pol. J. Environ. Stud.* 2021, 30, 1801–1808. <https://doi.org/10.15244/pjoes/125765>.
13. Mesnoua, M.; Remmani, R.; Benchik, C. Characterization of slow pyrolysis biochars from date palm residues with the aim of soil amendment. *J. Environ. Manag.* 2021, 247, 1–8.
14. Zhou, Y.; Qin, S.; Verma, S.; Sar, T.; Sarsaiya, S.; Ravindran, B.; Awasthi, M. K. Production and beneficial impact of biochar for environmental application: a comprehensive review. *Bioresour. Technol.* 2021, 337, 125451. <https://doi.org/10.1016/j.biortech.2021.125451>.
15. Remmani, R. Optimization and Application of Date Palm Seed Derived Biochar for Augmented Adsorption of Volatile Organic Compounds: A Specialized Inquiry into Trichloroethylene (TCE) and Tetrachloroethylene (PCE) Remediation. Doctoral Dissertation, Université Mohamed Khider (Biskra-Algérie) 2024. <http://dx.doi.org/10.13140/RG.2.2.26833.95848>.
16. Nunes, C.A.; Guerreiro, M.C. Estimation of surface area and pore volume of activated carbons by methylene blue and iodine numbers. *Quim. Nova* 2011, 34, 472–476. <https://doi.org/10.1590/S0100-40422011000300020>.
17. Amalina, F.; Krishnan, S.; Zularisam, A. W.; Nasrullah, M. Recent advancement and applications of biochar technology as a multifunctional component towards sustainable environment. *Environ. Dev.* 2023, 46, 100819. <https://doi.org/10.1016/j.envdev.2023.100819>.
18. Ho, Y.S.; McKay, G. Pseudo-second order model for sorption processes. *Process Biochem.* 1999, 34, 451–465. [https://doi.org/10.1016/S0032-9592\(98\)00112-5](https://doi.org/10.1016/S0032-9592(98)00112-5).
19. Roumani, M.; Remmani, R.; Miladi, M.; Abu-Khalaf, N.; Canales, A. R. Physical properties and mass models of Deglet Noor and Arichti semi-dry Algerian date fruits: A comparative study. *Food Sci. Nutr.* 2024, 12, 2886–2895. <https://doi.org/10.1002/fsn3.3969>.
20. Rossi, M. M.; Silvani, L.; Amanat, N.; Petrangeli Papini, M. Biochar from pine wood, rice husks and iron-eupatorium shrubs for remediation applications: Surface characterization and experimental tests for trichloroethylene removal. *Materials* 2021, 14, 1776. <https://doi.org/10.3390/ma14071776>.
21. U.S. Environmental Protection Agency. Definition and Procedure for the Determination of the Method Detection Limit, Revision 2. (EPA 821-R-16-006). U.S. Environ. Prot. Agency 2016.

Disclaimer/Publisher’s Note: The statements, opinions and data contained in all publications are solely those of the individual author(s) and contributor(s) and not of MDPI and/or the editor(s). MDPI and/or the editor(s) disclaim responsibility for any injury to people or property resulting from any ideas, methods, instructions or products referred to in the content.